Catalytic Conversion of Hydrocarbons and Formation of Carbon Nanofilaments in Porous Pellets
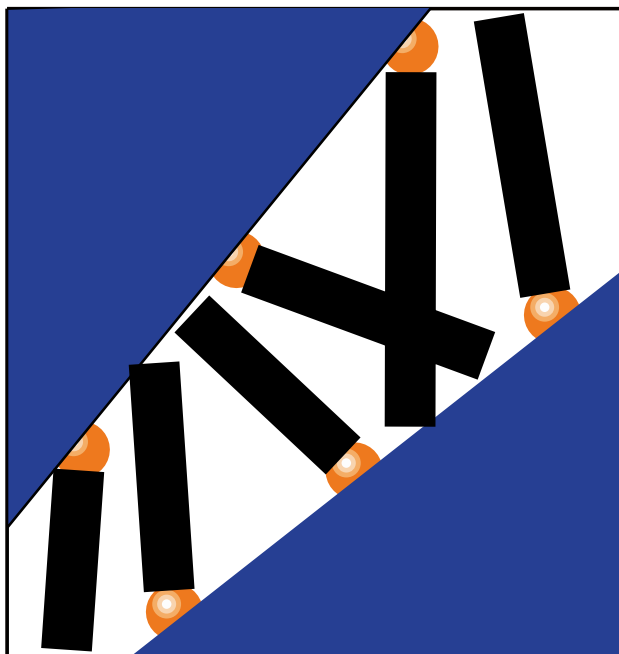
Vladimir P. Zhdanov[1,2]

Abstract

Catalytic conversion of hydrocarbons occurring at metal nanoparticles in porous pellets is often accompanied by the formation of coke in the form of growing heterogeneous film-like aggregates or carbon nanofilaments. The latter processes result in deactivation of metal nanoparticles. The corresponding kinetic models imply the formation and growth of film-like coke aggregates. Herein, I present an alternative generic kinetic model focused on the formation and growth of carbon nanofilaments. These processes are considered to deactivate metal nanoparticles and reduce the rate of reactant diffusion in pores. In this framework, the kinetically limited reaction regime is described by simple analytical expressions. The diffusion-limited regime can be described as well but only numerically. The model presented can be used for interpretation of experimental results.

Graphical Abstract

✉ Vladimir P. Zhdanov
  zhdanov@chalmers.se

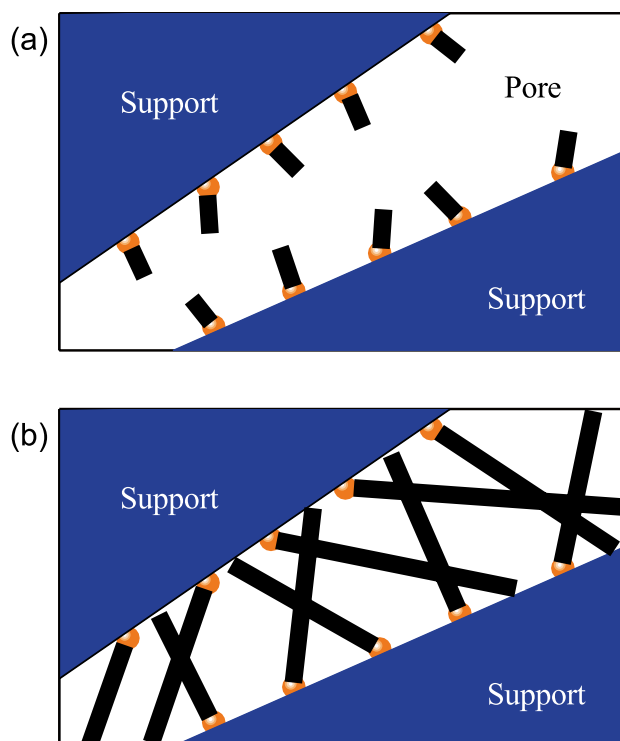Extended author information available on the last page of the article

1 Introduction

Many practically important heterogeneous catalytic reactions occurring with participation of hydrocarbons at metal nanoparticles (MNPs) in nanoporous supports are accompanied by the formation of coke which not only directly reduces the activity of MNPs but also suppresses the diffusion-mediated reactant supply via pores so that there is need in regeneration of a catalyst from time to time [1]. Mechanistically, the coke formation and removal are complex processes representing interesting examples of the interplay between reaction, diffusion, and blocking or opening of pores. In particular, the corresponding pathways of the catalyst deactivation embrace (i) carbon chemisorption at MNPs hindering the access of reactants, (ii) MNP encapsulation by coke, (iii) pore plugging by coke in the form of growing heterogeneous film-like aggregates or carbon nanofilaments (CNFs), and (iv) degradation of the porous support structure due to e.g. massive growth CNFs [2]. Each of these processes can be divided into its own steps and substeps and may occur via various scenarios. Taken together, such phenomena can physically be classified as a special type of percolation (for more conventional percolation, see [3] and references therein).

The understanding of the interplay of various processes running during the coke formation and removal is still limited, and the corresponding kinetic models are highly coarse-grained. The early models of coke formation are reviewed in [4–6]. Examples of recent models of this category can be found in Refs. [7–11] and [12–14] focused on coke formation and removal, respectively. In all these models, coke is viewed as a continuous expanding or shrinking film located at the walls of nanopores. There are also generic self-consistent coarse-grained Monte Carlo simulations of coke formation and removal at the level of the pore network [15]. Herein, I present an alternative generic kinetic model of the coke-mediated catalyst deactivation occurring via the CNF formation and growth on MNPs (as schematically shown in Fig. 1). The analysis is focused on the case when the main reaction and coke formation take place in a spherically shaped nanoporous pellet.

The details of how to describe the deactivation of MNPs in a porous pellet depends on whether the main reaction runs in the kinetically or diffusion-limited regime. In the absence of coke, these regimes can be illustrated in the framework of the classical Thiele model describing the first-order reaction running in a spherically shaped pellet [16] (briefly reviewed in [1, 15]). According to this model, the reactant concentration inside pores and the reaction effectiveness factor quantifying the role of diffusion are given by

$$\frac{c(r)}{c(R)} = \frac{R \sinh(r/\lambda)}{r \sinh(R/\lambda)} \quad \text{and} \quad \eta = \frac{3}{\phi}\left[\frac{\cosh \phi}{\sinh \phi} - \frac{1}{\phi}\right], \tag{1}$$

Fig. 1 Scheme of the growth of carbon nanofibers or nanotubes in nanopores on supported catalytic metal nanoparticles: (a) Initial and (b) late phases with the length of CNFs (nanofibers or nanotubes) much shorter and comparable with the pore diameter. During further growth of CNFs, their shape can be more complex, and the related strain can result in the formation of additional pores and subsequent degradation of catalyst structure [2] (in the model under consideration, the latter process is not taken into account). In this scheme, MNPs are considered to remain at the pore walls during the CNF growth. In some systems, CNFs grow with a MNP on their top [2]

where r is the radial coordinate, R is the pellet radius, $\lambda \equiv (D_e/k_e)^{1/2}$ is the scale of the diffusion length, and $\phi = (k_e R^2/D_e)^{1/2}$ is the corresponding modulus, whereas k_e and $D_e = (\epsilon/\tau)D_m$ are the effective reaction rate constant and diffusion coefficient (D_m is the molecular diffusion coefficient, and ϵ and τ are the porosity and tortuosity factors [17]). If diffusion is rapid ($\phi \ll 1$), the reactant distribution in pellets is nearly uniform so that $\eta \simeq 1$. If diffusion is slow ($\phi \gg 1$), the reactant concentration is relatively high near the external pellet-gas interface and drops inside so that $\eta \simeq 3/\phi \ll 1$.

Below, I first analyze theoretically the first-order reaction and CNF growth at a single MNP (Sec. 2) and then locally (Sec. 2) and globally (Secs. 3 and 4) in a spherically shaped pellet in the kinetically and diffusion-limited regimes under isothermal conditions. Some of the elements of my analysis are standard. Taken together, the treatment presented is, however, novel. Concerning the latter aspect, I can notice that the formation of filamentous coke is inherent to catalytic reactions occurring on base transition MNPs (Ni, Co

and Fe) in porous supports, although there are a few related reports on noble metals MNSs (Rh, Pt, and Ru) as well [2]. The kinetic models describing diffusion-influenced reactions complicated by the CNF growth are however lacking. In the absence of reaction, the CNF growth at MNPs on flat supports has been extensively studied experimentally and theoretically (see, e.g., reviews focused on carbon nanotubes [18, 19]). The corresponding models were, however, not used to describe reaction kinetics.

2 Local Reaction and CNF Growth

Phenomenologically, the CNF growth at a single MNP can be divided into two steps including nucleation and growth itself [20]. In particular, the CNF nucleation can be viewed as a process of reversible attachment and detachment of C atoms up to the formation of a critical nucleus [20]. By analogy with the conventional nucleation (reviewed e.g. in [21]), the CNF nucleation occurring at time t on a MNP located at the pore wall inside a pellet at coordinate r can be (i) characterized in terms of the corresponding probability $p(r, t)$, (ii) viewed as a first-order process with respect to this probability or, in other words, as a Poisson process (reviewed e.g. in [22]), and (iii) described as

$$dp(r,t)/dt = \kappa c^n(r,t)[1 - p(r,t)], \tag{2}$$

where κ is the nucleation rate constant, $c(r, t)$ is the local reactant concentration [as in (1)], and n is the kinetic order with respect to this concentration. The integration of this equation yields

$$p(t,r) = 1 - \exp\left(-\int_0^t \kappa c^n(r,\tau)d\tau\right). \tag{3}$$

The CNF growth after nucleation can be described in the spirit of the kinetic models used earlier for the growth of carbon nanotubes at a flat surface (see e.g. [23, 24]). In particular, the equation for the length of a CNF nucleated at time t' is

$$dl(r,t,t')/dt = \gamma c^m(r,t)[l_* - l(r,t',t)], \quad \text{or} \tag{4}$$

$$l(r,t,t') = l_*\left[1 - \exp\left(-\int_{t'}^t \gamma c^m(r,\tau)d\tau\right)\right], \tag{5}$$

where γ and m are the corresponding growth-rate constant and kinetic order, and l_* is the maximal length determined by the spatial constraints on the growth. At a flat surface, the spatial constraints are related to CNFs themselves, and l_* is large (e.g., ~ 1 mm [23, 24]). In the case under consideration, the CNF growth is complicated by the spatial

constraints in nanopores as well, and l_* is expected to be much shorter than 1 mm.

After nucleation, a part of the MNP remains active [2]. At the simplest level, this can be described by introducing the reaction rate constants before and after nucleation, k and k_*. Then, focusing on the first-order reaction [as in (1)], the local reaction rate, i.e., the reaction rate averaged over many MNPs can be represented as

$$w(r,t) = kc(r,t)[1 - p(r,t)] + k_*c(r,t)p(r,t). \tag{6}$$

Depending on the definition, k and k_* can characterize the reaction rate per MNP or per unit volume of the catalyst. Below, I use the latter definition.

In addition, it is convenient to introduce the volume of CNFs per unit volume of the pellet,

$$v(r,t) = c_\star \int_0^t \pi\rho^2 l(r,t,t')\frac{dp(r,t')}{dt'}dt', \tag{7}$$

where ρ is the CNF radius, and $c_\star$ is the local MNP concentration. In combination with (2), this equation results in

$$v(r,t) = \pi\rho^2 c_\star \int_0^t l(r,t,t')\kappa c^n(r,t')[1 - p(r,t')]dt'. \tag{8}$$

To describe the whole process, the equations introduced above should be combined with those for calculation of the reactant distribution in a pellet.

3 Kinetically Limited Reaction Regime

If the reaction runs in the kinetically limited regime, the gradients in $c(r, t)$ are negligible, i.e., $c(r, t)$ can be considered to be constant, i.e., independent of r and t. In this case, $p(r, t)$, $w(r, t)$, and $v(r, t)$ depend only on t, whereas $l(r, t, t')$ depends only on t and t'. Under these conditions, Eqs. (3), (5), (6) and (8) are reduced to
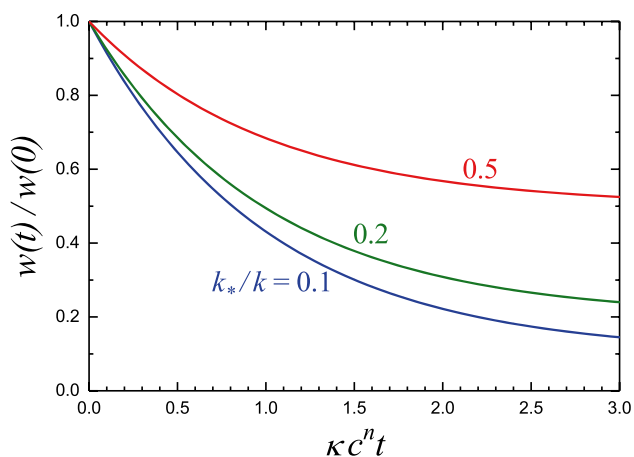
$$p(t) = 1 - \exp(-\kappa c^n t), \tag{9}$$

$$l(t,t') = l_*\{1 - \exp[-\gamma c^m(t - t')]\}, \tag{10}$$

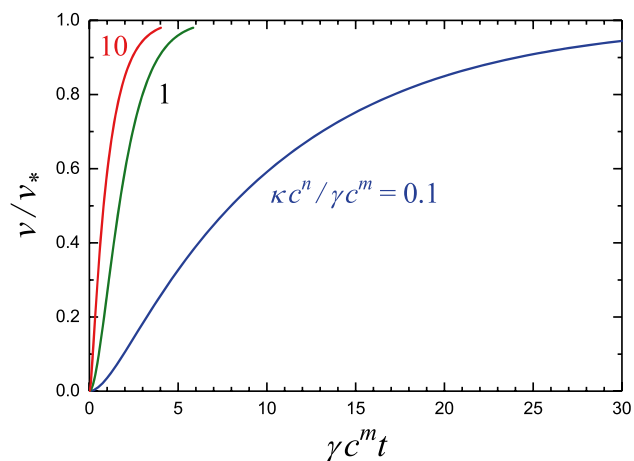$$w(t) = kc\exp(-\kappa c^n t) + k_*c[1 - \exp(-\kappa c^n t)], \tag{11}$$

$$v(t) = \pi\rho^2\kappa c_\star c^n \int_0^t l(t,t')[1 - p(t')]dt'. \tag{12}$$

Then, Eq. (12) in combination with (9) and (10) yield

$$v(t) = c_\star\pi\rho^2 l_*\kappa c^n \int_0^t \{1 - \exp[-\gamma c^m(t - t')]\}\exp(-\kappa c^n t')dt', \tag{13}$$

Fig. 2 Normalized reaction rate as a function of $\kappa c^n t$ in the kinetically limited reaction regime with $k_*/k = 0.1$, 0.2, and 0.5 [according to Eq. (11)]

Fig. 3 Normalized volume of growing CNFs as a function of $\gamma c^m t$ in the kinetically limited reaction regime with $\kappa c^n / \gamma c^m = 0.1$, 1, and 10 [according to Eq. (14)]. In these cases, the nucleation of CNFs is slow, moderate, and rapid, respectively

or

$$\frac{v(t)}{v_*} = 1 - \exp(-\kappa c^n t) - \frac{\kappa c^n [\exp(-\gamma c^m t) - \exp(-\kappa c^n t)]}{\kappa c^n - \gamma c^m}, \tag{14}$$

where $v_* \equiv \pi \rho^2 l_* c_\star$ is the maximal volume of CNFs. If the CNF nucleation is slow ($\kappa c^n \ll \gamma c^m$), the latter equation can be simplified as

$$v(t)/v_* \simeq 1 - \exp(-\kappa c^n t). \tag{15}$$

If the CNF growth is slow ($\kappa c^n \gg \gamma c^m$), it can be reduced to

$$v(t)/v_* \simeq 1 - \exp(-\gamma c^m t). \tag{16}$$

Typical kinetics predicted by Eqs. (11) and (14) are shown in Figs. 2 and 3.

4 Diffusion-Limited Reaction Regime

In the absence of coke, the diffusion-influenced transient kinetics of heterogeneous catalytic reactions occurring in porous spherically shaped pellets are usually described as

$$\epsilon \frac{\partial c(r,t)}{\partial t} = \frac{D_e}{r^2} \frac{\partial}{\partial r} \left(r^2 \frac{\partial c(r,t)}{\partial r} \right) - w(r,t), \tag{17}$$

where, as already mentioned in the Introduction,

$$D_e = \frac{\epsilon}{\tau} D_m \tag{18}$$

is the coordinate- and time-independent effective diffusion coefficient (D_m, ϵ, and τ are the corresponding molecular diffusion coefficient and porosity and tortuosity factors, respectively).

If the reaction is accompanied by the coke formation, it reduces the porosity and, in combination with diffusion limitations, results in the dependence of the effective diffusion coefficient on r and t. Under these conditions, Eqs. (17) and (18) should be modified as

$$\epsilon \frac{\partial c(r,t)}{\partial t} = \frac{1}{r^2} \frac{\partial}{\partial r} \left(r^2 D_e(r,t) \frac{\partial c(r,t)}{\partial r} \right) - w(r,t), \tag{19}$$

$$D_e(r,t) = \frac{\epsilon(r,t)}{\tau(r,t)} D_m(r,t). \tag{20}$$

Concerning expression (20), I can notice that D_m depends on r and t provided the diffusion is of the Knudsen type or close to this type, because in this case, D_m depends on the size and structure of pores. τ depends on r and t as well for the same reason. In the case of pores filled by CNFs, both these dependencies are complex and the corresponding analytical expressions are lacking. In contrast, the dependence of ϵ on r and t can analytically be described as

$$\epsilon(r,t) = \epsilon_o - v(r,t), \tag{21}$$

where ϵ_o is the porosity in the absence of coke [as in Eq. (18) except the subscript which has been added in order to indicate that this is the porosity at $t = 0$], and $v(r,t)$ is the dimensionless volume defined by (8).

On the timescale of coke formation, the reaction is rapid, and accordingly Eq. (19) can be solved in the steady-state approximation. Using this approximation and Eq. (6) for the reaction rate, Eq. (19) can be replaced by

$$\frac{1}{r^2}\frac{\partial}{\partial r}\left(r^2 D_e(r,t)\frac{\partial c(r,t)}{\partial r}\right) \tag{22}$$
$$= kc(r,t)[1 - p(r,t)] + k_* c(r,t)p(r,t).$$

This equation contains t as a parameter and should be integrated numerically at any given t with the conventional boundary equations,

$$c(R,t) = c_\circ \quad \text{and} \quad \left.\frac{\partial c(r,t)}{\partial r}\right|_{r=0} = 0, \tag{23}$$

where $c_\circ$ is the reactant concentration at the pellet boundary. Then, one can calculate the increment of $p(r,t)$ by employing Eq. (3). This procedure should be prolonged step by step.

Eqs. (19)-(23) make it possible to describe various situations. Their use is, however, complicated by the abundance of the parameters and some uncertainty in the dependence of τ on the amount of coke. The full-scale application of Eqs. (19)-(23) makes sense in order to interpret specific experimental studies providing detailed information reaction kinetics and CNF formation. In fact, such detailed studies are still lacking (reviewed in [2]).

Under such circumstances, I will use Eqs. (19)-(23) only for brief discussion of what may happens asymptotically at $t \to \infty$. In this limit, the model predicts that the reaction goes extinct, i.e. $w \to 0$, provided (i) the CNF formation fully deactivate a MNP (i.e., $k_* = 0$) and/or (ii) CNFs are able to fill all the porous space. Mathematically, the latter means $v(r,t) \to \epsilon_\circ$ and $D_e(r,t) \to 0$ [Eqs. (20) and (21)], and accordingly the diffusion-mediated reactant supply is fully suppressed. Physically, however, CNFs are not expected to be able to fill all the porous space (see, e.g., typical CNF snapshots in [2]). This means that $D_e(r,t)$ is expected to drop down to some finite value, $D_e(r,t) \to D_*$ at $t \to \infty$. In turn, the reaction rate constant can drop down to a finite value, $k_* > 0$, at $t \to \infty$ as well [Eq. (6)]. With this specification at $t \to \infty$, the model proposed will be equivalent to the Thiele model (see the Introduction) with the corresponding reaction rate constant, k_*, and reactant diffusion coefficient, D_*, and accordingly, with these parameters, the reactant concentration inside pores and the reaction effectiveness factor quantifying the role of diffusion will be given by Eq. (1).

5 Conclusion

I have presented a generic model describing the kinetics of catalytic reaction occurring on MNPs in a spherically shaped porous pellet and accompanying by the formation and growth of CNFs. The latter processes deactivate MNPs and reduce the rate of reactant diffusion in pores. In this framework, the kinetically limited reaction regime

is described by simple analytical expressions (Sec. 3). The diffusion-limited regime can be described as well (Sec. 4) but only numerically. The model presented can be used for interpretation of experimental results and also as a basis for developing more advanced models of the kinetics of catalytic reactions accompanying by the CNF formation and growth.

References

1. Thomas JM, Thomas WJ (2015) Principles and practice of heterogeneous catalysis. Wiley, Weinheim
2. Ochoa A, Bilbao J, Gayubo AG, Castano P (2020) Coke formation and deactivation during catalytic reforming of biomass and waste pyrolysis products: a review. Renew Sustain Energy Rev 119:109600
3. Xun Z, Hao D, Ziff RM (2022) Site and bond percolation thresholds on regular lattices with compact extended-range neighborhoods in two and three dimensions. Phys Rev E 105:024105
4. Froment GF (2008) Kinetic modeling of hydrocarbon processing and the effect of catalyst deactivation by coke formation. Catal Rev 50:1–18
5. Mann R (1997) Catalyst deactivation by coke deposition: approaches based on interactions of coke laydown with pore structure. Catal Today 37:331–349
6. Zhdanov VP (1993) Application of percolation theory to describing kinetic processes in porous solids. Adv Catal 39:1–50
7. Ye G et al (2019) Pore network modeling of catalyst deactivation by coking, from single site to particle, during propane dehydrogenation. AIChE J 65:140–150
8. Li H, Yuan X, Gao M, Ye M, Liu Z (2019) Study of catalyst coke distribution based on population balance theory: application to methanol to olefins process. AIChE J 65:1149–1161
9. Lin Y, Yang C, Choi C, Zhang W, Machida H, Norinaga K (2021) Lattice Boltzmann simulation of multicomponent reaction-diffusion and coke formation in a catalyst with hierarchical pore structure for dry reforming of methane. Chem Eng Sci 229:11610

10. Lei T, Liu X, Pathak AD, Shetty S, Liu Q, Wen X (2021) Insights into coke formation and removal under operating conditions with a quantum nanoreactor approach. J Phys Chem Lett 12:9413–9421

11. Yang X, Wang S, Zhang K, He Y (2021) Investigation of coke deposition inside catalyst with heterogeneous active component distribution. Fuel 287:119547

12. Ochoa A, Ibarra A, Bilbao J, Arandes JM, Castaño P (2017) Assessment of thermogravimetric methods for calculating coke combustion-regeneration kinetics of deactivated catalyst. Chem Eng Sci 171:459–470

13. Zhao J, Zhou J, Ye M, Liu Z (2020) Kinetic study on air regeneration of industrial methanol-to-olefin catalyst. Ind Eng Chem Res 59:11953–11961

14. Reshetnikov SI, Petrov RV, Zazhigalov SV, Zagoruiko AN (2020) Mathematical modeling of regeneration of coked Cr-Mg catalyst in fixed bed reactors. Chem Eng J 380:122374

15. Zhdanov VP (2022) Kinetics and percolation: coke in heterogeneous catalysts. J Phys A 55:174005

16. Thiele EW (1939) Relation between catalytic activity and size of particle. Ind Eng Chem 31:916–920

17. Rout KR, Jakobsen HA (2013) A numerical study of pellets having both catalytic- and capture properties for SE-SMR process: kinetic- and product layer diffusion controlled regimes. Fuel Process Technol 106:231–246

18. Rao R et al (2018) Carbon nanotubes and related nanomaterials: critical advances and challenges for synthesis toward mainstream commercial applications. ACS Nano 12:11756–11784

19. Li Y (2021) Carbon nanotube research in its 30th year. ACS Nano 15:9197–9200

20. Ding F, Bolton K, Rosén A (2004) Nucleation and growth of single-walled carbon nanotubes: a molecular dynamics study. J Phys Chem B 108:17369–17377

21. Kalikmanov VI (2013) Nucleation Theory, Sec. 15.7. Springer, Heidelberg

22. Fichthorn KA, Weinberg WH (1991) Theoretical foundations of dynamical Monte Carlo simulations. J Chem Phys 95:1090–1096

23. Futaba DN, Hata K, Yamada T, Mizuno K, Yumura M, Iijima S (2005) Kinetics of water-assisted single-walled carbon nanotube synthesis revealed by a time-evolution analysis. Phys. Rev. Lett. 95:056104

24. Bedewy M, Meshot ER, Reinker MJ, Hart AJ (2011) Population growth dynamics of carbon nanotubes. ACS Nano 5:8974–8989

Authors and Affiliations

Vladimir P. Zhdanov[1,2]

1 Section of Chemical Physics, Department of Physics, Chalmers University of Technology, Göteborg, Sweden

2 Boreskov Institute of Catalysis, Russian Academy of Sciences, Novosibirsk, Russia